Catalysis Today 172 (2011) 53–57

Contents lists available at ScienceDirect

Catalysis Today

journal homepage: www.elsevier.com/locate/cattod

$La_{1-x}Ca_xMnO_3$ perovskites as catalysts for total oxidation of volatile organic compounds

Walter P. Stege, Luis E. Cadús, Bibiana P. Barbero*

Instituto de Investigaciones en Tecnología Química (INTEQUI), UNSL-CONICET, Chacabuco 917, San Luis D5700BWS, Argentina

ARTICLE INFO

Article history:
Received 30 November 2010
Received in revised form 21 February 2011
Accepted 28 February 2011
Available online 9 April 2011

Keywords:
Ethanol
n-Hexane
Combustion
VOC
TPR
O_2-TPD

ABSTRACT

$La_{1-x}Ca_xMnO_3$ perovskites were prepared by the citrate method and characterized by means of X-ray diffraction, temperature programmed desorption of oxygen, temperature programmed reduction, and measurement of specific surface area. The characterization results indicated that pure perovskite phases were obtained and their specific surface areas are appropriate for the application in catalytic oxidation. The unsubstituted perovskite, $LaMnO_3$, could present a certain amount of Mn^{4+} and cationic vacancies, which is generally called oxidative nonstoichiometry. The electronic unbalance yield by the partial substitution of lanthanum by calcium, a cation of lower oxidation state, caused an oxidation state increase of part of the manganese occupying the B sites of the structure. Concurrently, the amount of cationic vacancies decreased with the increase of calcium amount. The catalytic activity was evaluated in the combustion of ethanol and n-hexane. Both reactions would occur by means of a suprafacial reaction mechanism in which the adsorbed oxygen species are relevant.

1. Introduction

An increasing interest has been shown in catalytic combustion processes during the last decades since they are a convenient way for emission prevention (the control of nitrogen oxides NO*x* and unburned hydrocarbons in heat and power generation plants) as well as clean-up (volatile organic compounds removal, automobile exhaust converters) [1,2].

The noble metal based catalysts show high specific activity in oxidation reactions [3] but its utilization is limited due to the high volatility of the pure metals and their oxides, and because of sintering at moderate temperatures. Perovskite-type oxides display prominent catalytic activities in many fields such as the total oxidation of CO, methane, and volatile organic compounds. This activity, coupled with a high thermal stability, postulates pervoskite-type oxides as potential catalysts in substitution of very active noble metals such as Pt and Pd, which are more expensive and do not resist operating at high temperatures [4–7].

The general formula of perovskite oxides is ABO_3, where the 12-coordinatedA sites may be occupied by rare-earth, alkaline-earth, alkali or other large ions and the 6-coordinated B sites are usually filled with transition metal cations.A large number of metallic cations can occupy the A and the B sites. Furthermore, the great stability of the perovskite framework allows partial substitution at the A sites and/or the B sites giving compounds of formulae $(A_xA'_{1-x})(B_yB'_{y-1})O_3$. The substitutions modify the catalytic, redox and structural properties. The substitution at A site with ions having lower valence can allow the formation of structural defects such as anionic or cationic vacancies and/or a change in the oxidation state of the transition metal cation to maintain the electroneutrality of the compound [8,9]. When the oxidation state of B cation increases, the relative easiness of the redox process generates larger quantities of available oxygen at low temperature and the overall oxidation activity enhances. Moreover, the oxygen vacancies favor the catalytic activity in oxidation reaction because they increase the lattice oxygen mobility.

Perovskites with lanthanum in A site and transition metals in B site ($LaBO_3$) with B = Mn, Co, Fe, Ni have received much attention. Particularly, the partial substitution of lanthanum in $LaMnO_3$ by Sr, Ce, Hf, Ag, or Ca was reported to enhance the catalytic activity in full oxidation reaction of CO and hydrocarbons [10–15]. In previous studies of our group, the calcium substitution in A site of $LaCoO_3$ [16] and $LaFeO_3$ [17] has showed a beneficial effect on the catalytic performance in combustion of VOC.

The aim of this work is to synthesize a series of $LaMnO_3$ perovskites partially substituted in the A site by different calcium amounts and to characterize it in order to determinate the changes induced in the lattice. Then, a correlation between the catalytic activity in the combustion of volatile organic compounds (ethanol and n-hexane) and the physicochemical properties of the catalysts is searched.

* Corresponding author. Fax: +54 2652 426711.
E-mail address: bbarbero@unsl.edu.ar (B.P. Barbero).

0920-5861/$ – see front matter © 2011 Elsevier B.V. All rights reserved.
doi:10.1016/j.cattod.2011.02.062

2. Experimental

2.1. Catalysts preparation

$La_{1-x}Ca_xMnO_3$ perovskites with $x = 0$, 0.1, 0.2, and 0.3 were prepared by the citrate method [18]. $La(NO_3)_3{\cdot}6H_2O$ (Fluka), $Ca(NO_3)_2{\cdot}4H_2O$ (Fluka), $Mn(NO_3)_2{\cdot}4H_2O$ (Merck) and citric acid (Mallinckrodt) were used as reagents. The aqueous solutions of the metal nitrates were added to an aqueous solution of citric acid with a 10% excess over the number of ionic equivalents of cations. The resulting solution was concentrated slowly by evaporating water under vacuum in a rotavapor at 70 °C until the formation of a gel. This gel was dried in an oven, increasing slowly the temperature at 2.5 °C/h up to 130 °C to yield a solid amorphous citrate precursor. The obtained precursor was calcined in air at 700 °C for 2 h. The perovskite catalysts are expressed by $La_{1-x}Ca_xMnO_3$ where $x = 0$, 0.1, 0.2, and 0.3, although the actual composition may be non-stoichiometric in relationship to the oxygen and may not be of single phase.

2.2. Catalysts characterization

2.2.1. Inductively coupled plasma-optical emission spectroscopy (ICP-OES)

The elemental composition was determined by inductively coupled plasma optical emission spectroscopy (ICPOES) in a Baird ICP 2070, with the use of a 1 m-Czemy Turner monochromator with a holographic grating with 1800 grooves mm^{-1}. In each experiment, 10 mg of each catalyst was dissolved in 5% HCl solution. The reference solutions were prepared with La_2O_3, Mn_2O_3, and $CaCO_3$.

2.2.2. Specific surface area

The specific surface area (SSA) of the catalysts was calculated by the BET method from the nitrogen adsorption isotherms obtained at 77 K on samples outgassed at 250 °C using a Micromeritics Gemini V apparatus.

2.2.3. X-ray diffractometry (XRD)

XRD patterns were recorded at room temperature by using a Rigaku diffractometer, model Geigerflex, operated at 30 kV and 20 mA, employing Ni-filtered Cu Ka radiation ($\lambda = 0.15418$ nm). The data were collected in the (2θ) range from 10° to 90°. The crystalline phases were identified by reference to the PDF data employing standard spectra software.

2.2.4. Oxygen temperature-programmed desorption (O_2-TPD)

O_2-TPD experiments were performed in a quartz reactor using a TCD as detector. In each analysis, 500 mg samples were pre-treated with helium gas increasing the temperature from ambient temperature up to 700 °C at 10 °C min^{-1}. The samples were oxidised with a 20% O_2/He mixture at a total flow rate of 30 ml min^{-1} at 700 °C for 30 min. Then, they were cooled down to ambient temperature in the oxidising mixture and flushed by a stream of purified He for 30 min. The desorption was carried out in the same conditions as the pre-treatment, maintaining the temperature at 700 °C until the baseline of the chromatograph was stabilised.

2.2.5. Temperature-programmed reduction (TPR)

TPR experiments were performed in the same apparatus used for O_2-TPD employing 50 mg samples. The reducing atmosphere was a 5% H_2/N_2 mixture at a total flow rate of 30 ml min^{-1}. The temperature was increased at 10 °C min^{-1} from ambient temperature to 700 °C.

Table 1
Specific surface areas (S_{BET}) and bulk composition determined by ICP-OES.

Catalyst	S_{BET} (m^2/g)	Ca	La	Mn	O[b]
$LaMnO_3$	25.1		56.4 (57.4)	21.4 (22.7)	22.2 (19.8)
$La_{0.9}Ca_{0.1}MnO_3$	24.0	2.2 (1.7)[a]	52.4 (53.9)	21.4 (23.7)	24.0 (20.7)
$La_{0.8}Ca_{0.2}MnO_3$	25.7	3.4 (3.6)	51.9 (50.0)	22.2 (24.7)	22.5 (21.6)
$La_{0.7}Ca_{0.3}MnO_3$	21.8	4.9 (5.7)	46.0 (45.8)	26.5 (25.9)	22.6 (22.6)

[a] In parentheses, the nominal composition.
[b] Calculated as a balance: 100 – (La + Ca + Mn).

2.3. Catalytic activity

The catalysts (300 mg, 0.5–0.8 mm particle diameter) diluted with glass particles of the same size in a ratio 1:5 were tested in a fixed-bed tubular reactor (1 cm inner diameter) operated at atmospheric pressure. The catalytic bed was approx. 1 cm height. The feed was a VOC:O_2:He mixture of 1:20:79 molar ratio. The total flow rate was 100 ml min^{-1} measured at ambient temperature. The temperature, measured with a coaxial thermocouple, was increased from 100 °C to attain total conversion of VOC (ethanol or n-hexane). The data obtained at each temperature were the average of, at least, two steady-state measurements. The reactants and reaction products were alternately analysed on-line by gas chromatography using a Carbowax 20M/Chromosorb W column and a TCD as detector. The conversion of VOC, X (%), is defined as the percentage of VOC feed that has reacted, i.e.:

$$X(\%) = \frac{[\mathrm{VOC}]_{in} - [\mathrm{VOC}]_{out}}{[\mathrm{VOC}]_{in}} \times 100$$

The experimental error of the measurements is ±5%.

3. Results and discussion

The catalysts were prepared by the citrate method because it is recognized as an appropriate method to obtain pure solids since the precursor gel is highly homogeneous. Furthermore, specific surface areas adequate for materials to be used as catalysts in oxidation reactions are obtained since considerably lower calcination temperatures than those employed in ceramic methods are sufficient to obtain the suitable phase. The perovskites synthesized in this work have specific surface areas between 22 and 26 m^2/g (Table 1). These values are notably higher than those reached by other synthesis methods (1–11 m^2/g) [14,19]. The specific surface area decreases as the calcination temperature increases [16], so, in this work, the samples were calcined at 700 °C. This temperature assures a good structural stability under reaction conditions, since the total conversion of VOCs is achieved at much lower temperature. Elemental analysis results with regard to La, Ca, and Mn (Table 1) show that the chemical composition is fairly close to that used in the preparation of the samples.

The synthesis success of the $La_{1-x}Ca_xMnO_3$ perovkites is evaluated from the X-ray diffraction results and the bulk composition determined by ICP-OES. As it is shown in Fig. 1, all diffractograms present only the diffraction lines corresponding to the $LaMnO_3$ perovskite (PDF 75-0440). No segregated phase or contamination, such as La_2O_3, CaO, or manganese oxides, was detected. This indicates that a single phase perovskite was obtained for all samples, at least, until the detection limit of XRD.

The calcium inclusion in the $LaMnO_3$ perovskite structure causes necessarily structural and/or stoichiometric changes due to the difference of charge between the substituted lanthanum cation (+3) and the calcium cation (+2). This structural change is appreciable in the X-ray diffractograms where a shift of the diffraction lines towards higher 2θ angles with the increase of the calcium content is observed. This indicates a decrease of the

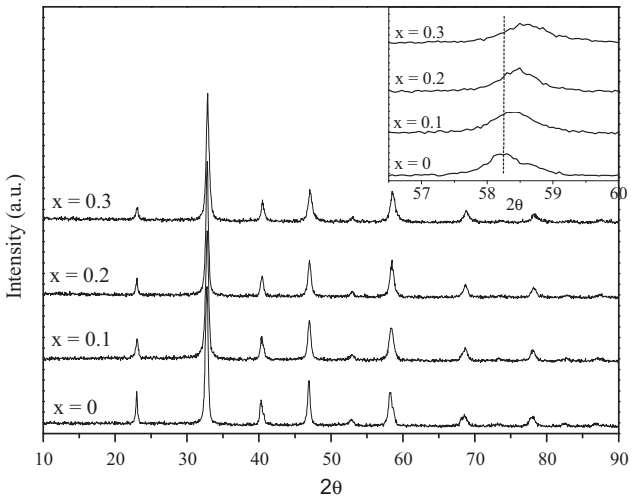

Fig. 1. Results of X-ray diffraction.

unit cell volume that could be originated by the difference of ionic radius of La^{3+} 12-coordinated (1.36 Å) with Ca^{2+} 12-coordinated (1.34 Å) [20]. However, this difference is very small and so; the cell volume should be very slightly affected by the calcium substitution. A very plausible modification that can justify the decrease of the cell volume is the increase of the oxidation state of the manganese occupying the B sites of the structure. In order to conserve the electroneutrality, a part of manganese can become Mn^{4+} which ionic radius (0.53 Å) is considerably smaller than that of Mn^{3+} (0.645 Å). The existence of Mn^{4+} has been detected in several $LaMnO_3$ perovskites substituted by Ca, Sr, Ce, Ag [12–15,19] and even in the unsubstituted perovskite [12–14,19]. In this last case, the electroneutrality principle is attained by means of an oxygen overstoichiometry, also called as oxidative nonstoichiometry, usually represented as $LaMnO_{3+\delta}$. It is important to note that the excess oxygen does not correspond to oxygen included into the perovskite structure, but it is a consequence of the cationic vacancies in the A and B sites [21]. A more correct expression for representing the oxidative nonstoichiometry is $A_x\phi_{1-x}B_y\Theta_{1-y}O_3$, where ϕ represents vacancies in the A site and Θ, vacancies in the B site. However, the $ABO_{3+\delta}$ nomenclature has been widely accepted by simplicity. In the last column of Table 1, the oxygen composition was calculated as a balance: 100–(La + Ca + Mn). The difference between these values and the nominal ones presented in parentheses is clearly observed in Fig. 2. This indicates that effectively the $La_{1-x}Ca_xMnO_3$

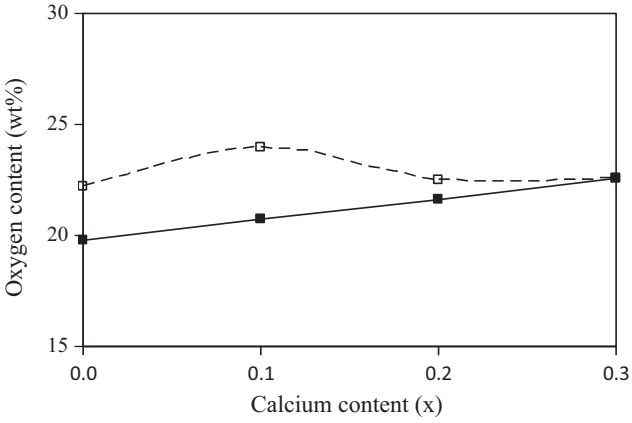

Fig. 2. Oxygen content as a function of the calcium content. (■) nominal; (□) calculated as a balance (last column of Table 1).

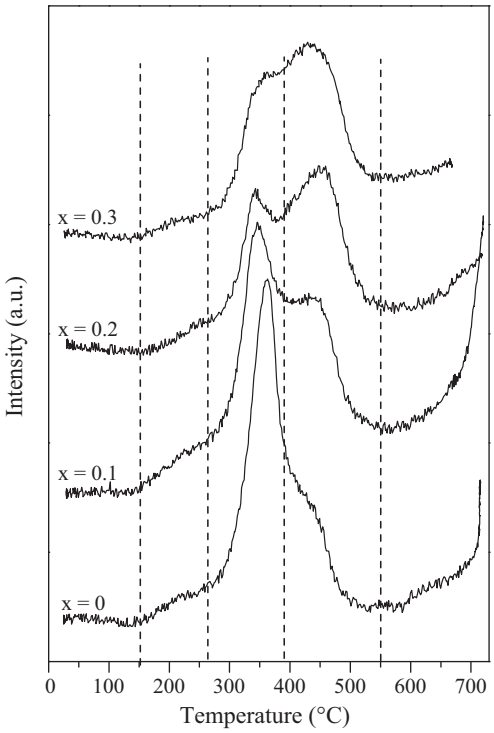

Fig. 3. Profiles of temperature programmed reduction.

with $x \leq 0.2$ exhibits an excess of oxygen and the amount decreases with the calcium content.

The temperature programmed reduction profiles may give information about the oxidation state of manganese and/or the existence of cationic vacancies. As it can be seen in Fig. 3, the TPR curves present a splitted signal with maxima at around 340–360 °C and 450 °C. Vogel et al. [22] observed in the TPR of $LaMnO_{3.13}$ a very stable intermediate reduced state in a range of 500–900 °C, corresponding to stoichiometric $LaMnO_3$. This implicates that the reduction signal below 500 °C is due to the elimination of the excess oxygen of the perovskite and the reduction of Mn^{4+} formed to compensate the electronic unbalance caused by Ca incorporation [11,12].

In our TPR curves of $La_{1-x}Ca_xMnO_3$ perovskites, two zones may be distinguished: (i) a zone between 260 °C and 390 °C which shows a well defined signal for $0 \leq x \leq 0.2$ with a slight shift of the maximum towards lower temperatures and a notable decrease of the intensity with the increase of x. For $x = 0.3$, the signal presents an intensity similar to $x = 0.2$ and it is overlapped with the following signal; and (ii) a zone between 390 °C and 550 °C which intensity increases with x. By analogy with that reported for cerium substituted lanthanum manganese perovskite [12], we propose that the signal between 260 °C and 390 °C corresponds to the removal of oxygen from a structure presenting oxidative nonstoichiometry (reaction (1)) while the signal between 390 °C and 550 °C represents the reduction of Mn^{4+} to Mn^{3+} (reaction (2)).

$$La_{1-x}Ca_xMn_{1-x-2\delta}{}^{3+}Mn_{x+2\delta}{}^{4+}O_{3+\delta} + \delta H_2 \rightarrow La_{1-x}Ca_xMn_{1-x}{}^{3+}Mn_x{}^{4+}O_3 + \delta H_2O \quad (1)$$

$$La_{1-x}Ca_xMn_{1-x}{}^{3+}Mn_x{}^{4+}O_3 + \tfrac{1}{2} \times H_2 \rightarrow La_{1-x}Ca_xMn^{3+}O_{3-x/2} + \tfrac{1}{2} \times H_2O \quad (2)$$

Above 550 °C, other reduction step starts which is not completed below 700 °C, the maximum temperature achieved in this study.

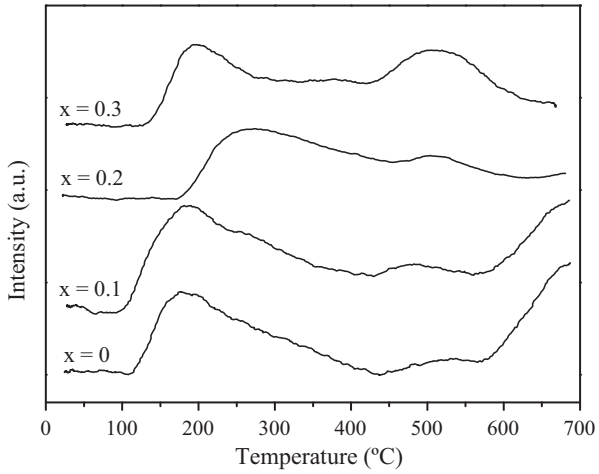

Fig. 4. Curves of temperature programmed desorption of oxygen.

In agreement with the information reported in literature [12,21], the signal at high temperature may be assigned to the reduction of Mn^{3+} to Mn^{2+} with the concurrent destruction of the perovskite structure (reaction (3)).

$$La_{1-x}Ca_xMn^{3+}O_{3-x/2} + ½H_2 \rightarrow ½(1-x)La_2O_3 + xCaO + MnO + ½H_2O \quad (3)$$

The intensity of the signal assigned to the reduction of Mn^{4+} (range from 390 °C to 550 °C) increases with the increase of the calcium content in agreement with the practically linear shift of the XRD lines (detail in Fig. 1). This indicates that the calcium has been completely introduced in the structure and an enough amount of Mn^{4+} has been generated in order to conserve the electroneutrality. Concurrently, the excess oxygen decreases with the calcium amount (range between 260 °C and 390 °C) in agreement with the prediction from the results of elemental composition (last column in Table 1).

Preceding the main reduction signal, a very weak signal between 150 °C and 260 °C can be distinguished. Taking into account that it occurs at relatively low temperature, it is feasible to think that this signal correspond to removal of oxygen from the surface layer or adsorbed oxygen on surface vacancies. With the aim to know about the existence of vacancies in the structure of the $La_{1-x}Ca_xMnO_3$ perovskites, studies of temperature programmed desorption of oxygen were performed. The curves of O_2-TPD (Fig. 4) show a very broad signal between 100 °C and 450 °C and other signal between 440 °C and 570 °C. In agreement with Seiyama [in 4, pp. 215], the signals at low temperature can be attributed to desorption of oxygen species adsorbed on surface vacancies and they are usually denoted as α oxygen species. As it has been observed in other perovskites-type oxides [23,24], our results exhibit two types of adsorbed oxygen species. The signal at low temperature (between 100 °C and 440 °C) can be attributed to the suprafacial adsorbed oxygen, while the oxygen released around 500 °C is considered as oxygen species occupying the inner vacancies created by substitution of La by Ca. Considering that the area under the curve is proportional to the amount of desorbed oxygen, it can be established that the amount of surface vacancies (signal between 100 °C and 440 °C) in the perovskites decreases in the order: $La_{0.9}Ca_{0.1}MnO_3 > LaMnO_3 \approx La_{0.7}Ca_{0.3}MnO_3 > La_{0.8}Ca_{0.2}MnO_3$. This intensity order is very similar to that of the reduction signal between 150 °C and 260 °C and therefore, can be suggested that the reduction signal at low temperature corresponds to adsorbed oxygen.

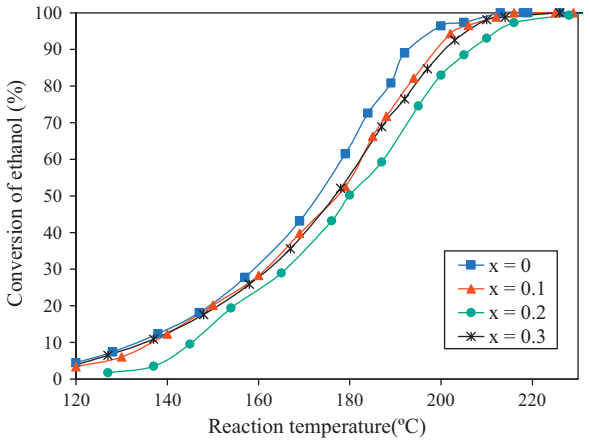

Fig. 5. Conversion of ethanol as a function of the reaction temperature.

For $x = 0$ and $x = 0.1$, a desorption signal begins around 570 °C but is not completed under the experimental conditions employed in this work. This desorption signal at high temperature is generally assigned to desorption of oxygen from the surface lattice and denoted as β oxygen species. They are correlated to the partial reduction of the B cation and therefore, in our catalysts, this signal could be associated to the excess oxygen.

It is expected that the modifications caused in the perovskites due to the partial substitution of La by Ca provoke an alteration of the catalytic behavior. In order to verify this assumption, the samples were evaluated in the combustion of two different molecules: an alcohol (ethanol) and an alkane (n-hexane). These compounds can be considered model molecules of volatile organic compounds and can present different behavior with a same catalytic system.

In Figs. 5 and 6, the curves of VOC conversion as a function of the reaction temperature are shown. As it is observed, the total conversion of ethanol is reached below 230 °C and for n-hexane, below 365 °C. These values show the high potentiality of the $La_{1-x}Ca_xMnO_3$ perovskites as catalysts for combustion since they are more active than pure Mn_2O_3 [25,26], a very active catalyst in oxidation reactions. In order to made a more adequate comparison of the catalytic performance, in Figs. 7 and 8, the intrinsic activity expressed as μmol of converted VOC per square meter (BET) and minute are presented. In the case of ethanol combustion, $La_{0.8}Ca_{0.2}MnO_3$ is markedly less active than the rest of the samples in the whole range of reaction temperature. The other perovskites, at reaction temperatures below 190 °C, have a similar intrinsic activity, within the experimental error,

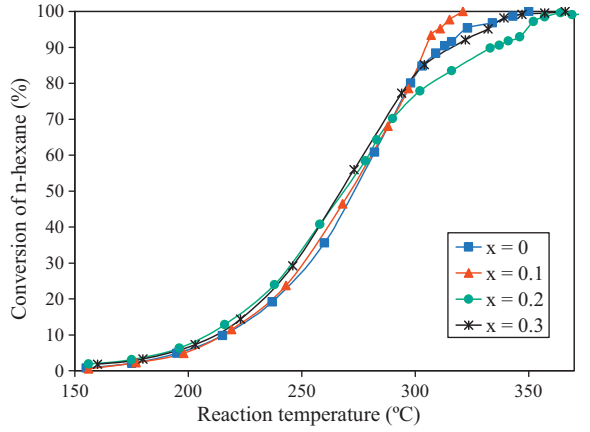

Fig. 6. Conversion of n-hexane as a function of the reaction temperature.

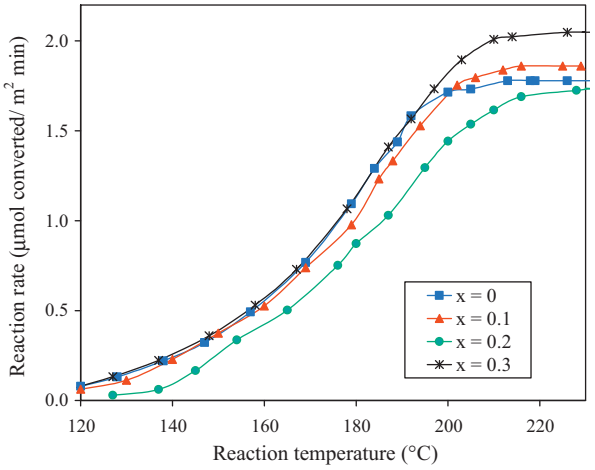

Fig. 7. Intrinsic activity in ethanol combustion as a function of the reaction temperature.

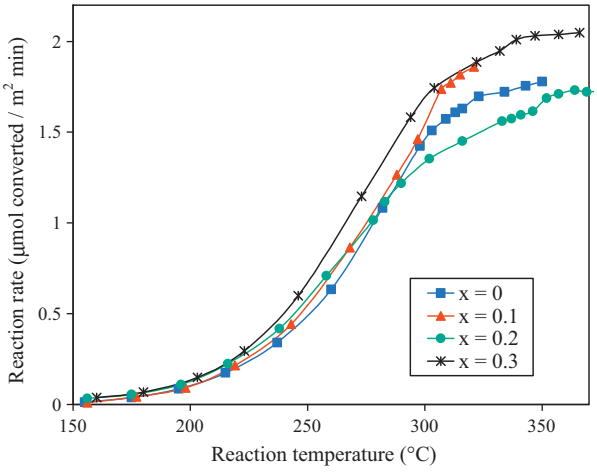

Fig. 8. Intrinsic activity in n-hexane combustion as a function of the reaction temperature.

and at reaction temperature above 200 °C, the reactivity order is: $La_{0.7}Ca_{0.3}MnO_3 > La_{0.9}Ca_{0.1}MnO_3 > LaMnO_3 > La_{0.8}Ca_{0.2}MnO_3$. These results can be explained correlating them with the O_2-TPD profiles. In Fig. 4, it can be observed that the maximum of the first desorption peaks for $LaMnO_3$, $La_{0.9}Ca_{0.1}MnO_3$, and $La_{0.7}Ca_{0.3}MnO_3$ is around 180–200 °C, while for $La_{0.8}Ca_{0.2}MnO_3$ the maximum is at 260 °C. This higher desorption temperature indicates more strongly adsorbed oxygen species [27] and consequently, less reactive oxygen. The difference of reactivity above 200 °C is in agreement with the amount of oxygen species releasing at around 500 °C.

In the case of n-hexane combustion, $La_{0.7}Ca_{0.3}MnO_3$ is the most active catalyst in the whole range of reaction temperature. The rest of the samples, at reaction temperature below 290 °C, presents a similar behavior, within the experimental error; while above 300 °C, the reactivity order is equal to that presented by the ethanol combustion. Again, this performance is in line with the O_2-TPD results although only the oxygen species released at around 500 °C are relevant in the reaction. This is expected considering that the n-hexane combustion occurs at higher temperature than the ethanol combustion. Therefore, it can be suggested that both the ethanol and n-hexane combustion occurs by means of a suprafacial reaction mechanism in which the adsorbed oxygen species play a predominant role.

4. Conclusions

Pure $La_{1-x}Ca_xMnO_3$ perovskites with specific surface areas appropriate to be used in catalytic oxidation reactions were obtained. The unsubstituted perovskite, $LaCaMnO_3$, presented a certain amount of Mn^{4+} and cationic vacancies, which is usually called as oxidative nonstoichiometry. The electronic unbalance provoked by the partial substitution of lanthanum by calcium, a lower oxidation state cation, caused an increase of the oxidation state of part of the manganese occupying the B sites in the structure. Concurrently, the amount of cationic vacancies decreased with the increase of the calcium content.

The catalytic activity was evaluated in the combustion of two molecules, ethanol and h-hexane, which are considered as volatile organic compound models. The total conversion was reached below 230 °C for ethanol combustion and 365 °C for n-hexane combustion. Both reactions would occur by means of a suprafacial mechanism in which the adsorbed oxygen species are relevant.

Acknowledgements

The authors thank the financial support from Universidad Nacional de San Luis, CONICET, and ANPCyT (Argentina).

References

[1] N. Mukhopadhyay, E.C. Moretti, Reducing and Controlling Volatile Organic Compounds, Centre for Waste Reduction Technologies, AIChE, New York, 1993.
[2] R.E. Heyes, S.T. Kolazkowski, Introduction to Catalytic Combustion, Gordon & Breach Science Publisher, Amsterdam, 1997.
[3] F.M.Z. Marcus, G.J. Sven, P.G. Menon, Catal. Rev. Sci. Eng. 35 (3) (1993) 319.
[4] L.G. Tejuca, J.L.G. Fierro (Eds.), Properties and Applications of Perovskite-type Oxides, Marcel Dekker, 1993.
[5] L. Simonot, F. Garin, G. Maire, Appl. Catal. B 11 (1997) 167.
[6] P. Ciambelli, S. Cimino, S. De Rossi, M. Faticanti, L. Lisi, G. Minelli, I. Pettiti, P. Porta, G. Russo, M. Turco, Appl. Catal. B 24 (2000) 243.
[7] H. Huang, Y. Liu, W. Tang, Y. Chen, Catal. Commun. 9 (2008) 55.
[8] L.G. Tejuca, J.L.G. Fierro, J.M.D. Tascón, Adv. Catal. 36 (1989) 237.
[9] T. Seiyama, Catal. Rev. Sci. Eng. 34 (1992) 281300.
[10] T. Nitadori, S. Kuriharam, M. Misono, J. Catal. 98 (1986) 221.
[11] S. Ponce, M.A. Peña, J.L.G. Fierro, Appl. Catal. B 24 (2000) 193.
[12] Y. Zhang-Steenwinkel, J. Beckers, A. Bliek, Appl. Catal. A 235 (2002) 79.
[13] A. Machocki, T. Ioannides, B. Stasinska, W. Gac, G. Avgouropoulos, D. Delimaris, W. Grzegorczyk, S. Pasieczna, J. Catal. 227 (2004) 282.
[14] N.H. Batis, P. Delichere, H. Batis, Appl. Catal. A 282 (2005) 173.
[15] J. Deng, Y. Zhang, H. Dai, L. Zhang, H. He, C.T. Au, Catal. Today 139 (2008) 82.
[16] N.A. Merino, B.P. Barbero, P. Grange, L.E. Cadús, J. Catal. 231 (2005) 232.
[17] B.P. Barbero, J. Andrade Gamboa, L.E. Cadús, Appl. Catal. B 65 (2006) 21.
[18] P. Courty, H. Ajot, C. Marcilly, B. Delmon, Power Technol. 7 (1973) 21.
[19] E.G. Vrieland, J. Catal. 32 (1974) 415.
[20] R.D. Shannon, Acta Cryst. A 32 (1976) 751.
[21] J. Töpfer, J.B. Goodenough, J. Solid State Chem. 130 (1997) 117.
[22] E.M. Vogel, D.W. Johnson, P.K. Gallagher, J. Am. Ceram. Soc. 60 (1977) 31.
[23] D. Ferri, L. Forni, Appl. Catal. B 16 (1998) 119.
[24] Z. Zhao, X. Yang, Y. Wu, Appl. Catal. B 8 (1996) 281.
[25] M.R. Morales, B.P. Barbero, L.E. Cadús, Appl. Catal. B 74 (2007) 1.
[26] F.G. Durán, B.P. Barbero, L.E. Cadús, C. Rojas, M.A. Centeno, J.A. Odriozola, Appl. Catal. B 92 (2009) 194.
[27] W. Wang, H. Zhang, G. Lin, Z. Xiong, Appl. Catal. B 24 (2000) 219.